RNAi-mediated TCR Knockdown Prevents Autoimmunity in Mice Caused by Mixed TCR Dimers Following TCR Gene Transfer

Mario Bunse[1,2], Gavin M Bendle[3,4], Carsten Linnemann[3], Laura Bies[3], Stephan Schulz[5], Ton N Schumacher[3] and Wolfgang Uckert[1,2]

[1]Max Delbrück Center for Molecular Medicine, Berlin, Germany; [2]Institute of Biology, Humboldt-Universität zu Berlin, Berlin, Germany; [3]Division of Immunology, The Netherlands Cancer Institute, Amsterdam, The Netherlands; [4]Current address: School of Cancer Sciences, University of Birmingham, Birmingham, UK; [5]Institute of Pathology, Charité Campus Mitte, Berlin, Germany.

Genetically modified T cells that express a transduced T cell receptor (TCR) α/β heterodimer in addition to their endogenous TCR are used in clinical studies to treat cancer. These cells express two TCR-α and two TCR-β chains that do not only compete for CD3 proteins but also form potentially self-reactive mixed TCR dimers, composed of endogenous and transferred chains. To overcome these deficits, we developed an RNAi-TCR replacement vector that simultaneously silences the endogenous TCR and expresses an RNAi-resistant TCR. Transduction of the virus-specific P14 TCR without RNAi resulted in unequal P14 TCR-α and -β chain surface levels, indicating heterodimerization with endogenous TCR chains. Such unequal expression was also observed following TCR gene optimization. Equal surface levels of the introduced TCR chains were however achieved by silencing the endogenous TCR. Importantly, all mice that received cells transduced with the native or optimized P14 TCR developed lethal TCR gene transfer-induced graft-versus-host-disease (TI-GVHD) due to formation of mixed TCR dimers. In contrast, TI-GVHD was almost completely prevented when using the RNAi-TCR replacement vector. Our data demonstrate that RNAi-assisted TCR replacement reduces the formation of mixed TCR dimers, and thereby significantly reduces the risk of TI-GVHD in TCR gene therapy.

Received 8 November 2013; accepted 17 July 2014; advance online publication 26 August 2014. doi:10.1038/mt.2014.142

INTRODUCTION

Transduction of T cell receptor (TCR) genes into T cells is an attractive approach to generate large pools of antigen-specific T cells for the treatment of cancer and infectious diseases.[1–4] The transfer of T cells targeting tumor-associated antigens can overcome the tolerance mechanisms that usually prevent immune reactions against such self antigen-derived epitopes.[5] Initial clinical studies have proven the feasibility of TCR gene therapy[6,7] and promising clinical responses have been observed.[8] However T cell transfer also bears the risk of autoimmunity if antigens are recognized on healthy tissue, either by cross reactivity of the introduced TCR with other epitopes (off-target toxicity), or by the expression of the targeted antigen in other tissues (on-target toxicity), with the latter already being observed in several clinical studies.[7,9,10]

Also, TCR gene transfer itself could induce off-target toxicity, because the expression of two pairs of TCR α/β genes allows the assembly of four different TCR α/β dimers: the endogenous TCR, the transferred TCR, and two mixed TCR dimers, composed of endogenous and transferred TCR chains. It has long been suspected that mixed TCR dimers may by chance recognize self-antigens as they are not subject to thymic selection.[11] Recently, it was reported that in an *in vitro* system, virus-specific human T cell lines became allo- and self-reactive after being transduced with an antigen-specific TCR[12] and that in an *in vivo* model of TCR gene therapy, mixed TCR dimers induced a lethal autoimmune pathology, termed TCR gene transfer-induced graft-versus-host disease (TI-GVHD).[13] Decreasing the amount of mixed TCR dimers expressed on gene-modified T cells by an advanced vector design and TCR gene optimization reduced TI-GVHD but did not completely prevent it in most cases.

In TCR gene-modified T cells, the TCR surface levels are the outcome of a competition between the endogenous and the transferred chains for heterodimerization and CD3 proteins. In this nonphysiological situation as yet undefined properties of the individual TCRs come into play and confer some TCRs an advantage over others.[14–16] As the outcome of the competition can be controlled by the TCR protein quantity, high-level TCR expression vectors have been developed using viral promoters,[17] linkage of both chains by a 2A element[18] and codon-optimized genes.[19] Another strategy is to engineer the TCR constant (C) regions to induce preferential pairing of transferred TCR chains.[20–25] For most TCRs, these strategies result in improved MHC multimer binding often accompanied by improved functionality. However, these two characteristics alone are not sufficient to conclude that mixed TCR dimers have been sufficiently reduced to prevent autoreactivity.

Correspondence: Wolfgang Uckert, Max Delbrück Center for Molecular Medicine, Robert-Rössle-Straße 10, 13092 Berlin, Germany. E-mail: wuckert@mdc-berlin.de

New strategies developed to minimize the risk of mixed TCR dimer-induced autoimmunity and maximize expression of the introduced TCR target the endogenous TCR directly. Artificial zinc-finger nucleases have been used to generate T cells with disrupted endogenous TCR genes[26] and retroviral vectors have been developed that simultaneously silence the endogenous TCR using RNA interference (RNAi) and express new RNAi-resistant TCR.[27–29] Whereas zinc-finger nucleases-mediated TCR gene editing is an appealing approach that completely shuts down TCR expression, the protocol requires ~40 days of *in vitro* T cell culture including multiple sorting steps. In contrast, RNAi-assisted TCR replacement uses a one-step transduction protocol, but may not completely deplete all TCR gene-modified T cells of endogenous TCR protein. Reduced endogenous TCR mRNA levels in human T cells have been successfully correlated with higher surface levels of a second RNAi-resistant TCR, but neither the amount of remaining endogenous TCR protein was determined nor if the transferred TCR chains reached endogenous surface expression levels. Since even low level expression of a second TCR induces mixed TCR dimer formation,[30] it remained unresolved whether the RNAi approach would reduce the formation of mixed TCR dimers, so that the generation of self-directed specificities in the population of transduced T cells is prevented. Therefore, we initiated a study to investigate how the reduction of endogenous TCR in TCR gene-modified T cells affects the development of mixed TCR dimer-dependent autoimmunity.

Here, we report that silencing of the endogenous TCR dramatically improved the survival of mice in a model of TCR gene therapy. To show this, we developed a γ-retroviral novel RNAi-TCR replacement vector for mouse T cells and determined the silencing efficiency on the protein level. TCR replacement was assessed by analyzing the surface levels of both transferred TCR chains, which predicted the amount of mixed TCR dimers better than MHC multimer binding. We present data indicating that the mitigation of the TCR competition by RNAi leads to equal surface levels of both transferred TCR chains and almost fully prevents otherwise lethal mixed TCR dimer-dependent autoimmunity in mice.

RESULTS

Intronic miRNA results in superior transgene expression compared with exonic miRNA

For two reasons, we employed a vector design that allows the expression of the RNAi triggers for the silencing of the endogenous TCR and of a therapeutic TCR by the same polymerase II promoter: first, both elements should be encoded by the same vector and, second, the expression of both elements should be firmly coupled. This vector design ensures that the TCR gene-modified T cells can be generated in a single transduction step and that the transferred TCR cannot be expressed without simultaneous silencing of the endogenous TCR. For this purpose, miRNAs are ideally suited as triggers of RNAi. We have generated a redirected mouse miRNA-155 (ref. 31) targeting the TCR Cα region and an artificial miRNA[32] targeting the TCR Cβ region, termed miRα and miRβ. Then, we modified a green fluorescent protein (GFP)-encoding γ-retroviral MP71 vector by the introduction of the miRβ either at one of two exonic positions 5′ and 3′ of the GFP or at one intronic position within the 5′ untranslated region (**Figure 1a**). All positions allowed the generation of functional miRNA as the surface TCR levels of transduced T cells were reduced by more than 90% compared to the control (**Figure 1b,c**). Furthermore, a linear relationship of GFP expression and TCR silencing was observed when the miRNA was located either at the 5′ intronic or the 3′ exonic position. However, the relative GFP levels ranged from 32% for the 5′ intronic position to 2% and 15% for the 5′ and the 3′ exonic positions, respectively (**Figure 1d**). Based on these data, we decided to use intronic miRNA for the design of the RNAi-TCR replacement vector. T cells stained for the CD3/TCR complex and transduced with vectors harboring either the miRα or the miRβ or both miRNAs (miR cassette) at the 5′ intronic position showed comparable silencing efficiencies of 16, 19, and 15%, respectively, and comparable relative GFP levels of 26, 34, and 28%, respectively (**Figure 1e–g**). These data demonstrate, that both miRNAs used for the silencing of the endogenous TCR chains were equally effective and that the introduction of a second miRNA did not lead to a further reduction of GFP expression.

Silencing of the endogenous TCR supports the expression of an RNAi-resistant second TCR

To analyze how the reduced transgene expression strength of the miRNA vectors influences their ability to express a second TCR in T cells and how the RNAi-mediated silencing of the endogenous TCR in turn supports the surface expression of a transferred TCR, we exchanged GFP for a P14 TCR cassette with silent mutations at the RNAi target sites (**Figure 2a**). This TCR recognizes the MHC class I-restricted GP33-41 epitope of lymphocytic choriomeningitis virus glycoprotein.[33] In T cells transduced with the miR cassette-encoding vector (miR-P14), only the net result can be measured on the cell surface. However, in cells transduced with vectors encoding a single miRNA, one of both P14 TCR chains is not supported by the RNAi effect. 62% of the cells expressed both P14 TCR chains (Vα2, Vβ8) at high levels after transduction with the miR-P14 vector, whereas the cells generated with similar transduction efficiencies using the single miRNA vectors expressed only one of the P14 TCR chains at a high level (**Figure 2b**). Only the P14 TCR chain was preferentially expressed whose endogenous counterpart was silenced by miRNA. Specifically, miRα-P14 vector-transduced cells showed relative Vα2 and Vβ8 chain levels of 76 and 41%, whereas miRβ-P14 vector-transduced cells showed relative Vα2 and Vβ8 chain levels of 16 and 117% (**Figure 2c**). Furthermore, we analyzed TCR-I transgenic T cells, which recognize the simian virus 40 large tumor antigen epitope I ($SV40_I$) presented by MHC class I,[34] that were transduced and stained for endogenous and transferred TCR using MHC multimers. Strikingly, transduction of the P14 vector without miR cassette resulted in cells that bound exclusively both MHC multimers, whereas transduction of the miR-P14 vector generated a high percentage of cells that stained only positive for the P14 TCR-specific multimer (**Supplementary Figure S2**). These data demonstrate, that the expression of the miR cassette resulted in simultaneous silencing of both endogenous TCR chains and that the low level of transgene expression of the miRNA vector could be compensated by the reduction of TCR competition in TCR gene-modified T cells.

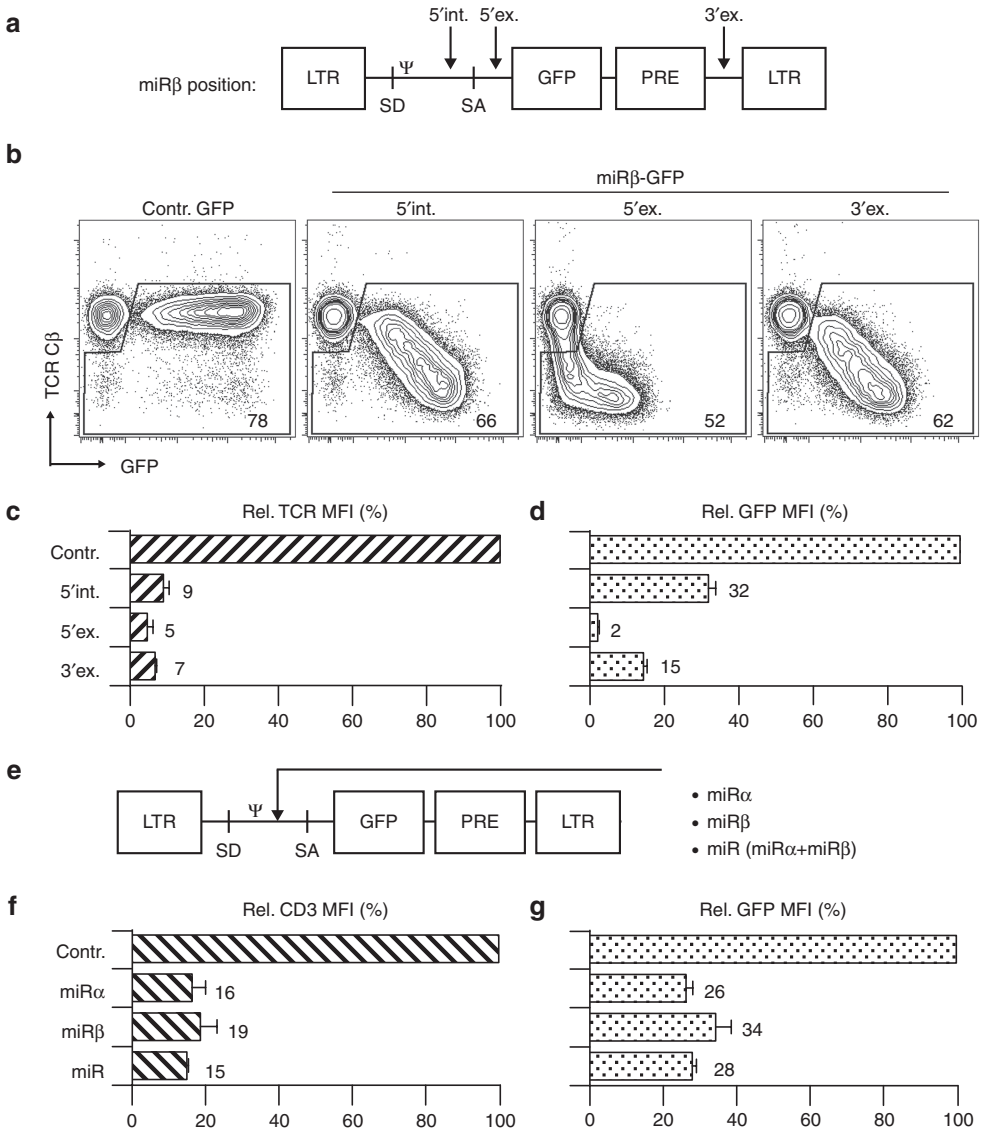

Figure 1 Intronic miRNA results in superior transgene expression compared with exonic miRNA. (**a**) A miRNA targeting the T cell receptor (TCR)-β chain (miRβ) was introduced into GFP-encoding MP71 vectors at following positions: 5′ intronic (5′ int.), 5′ exonic (5′ ex.) and 3′ exonic (3′ ex.). LTR, long terminal repeat; PRE, post-transcriptional regulatory element; SA, splice acceptor; SD, splice donor; Ψ, packaging signal. (**b**) TCR surface levels and GFP expression of transduced polyclonal splenocytes were determined by flow cytometry. The percentage of gated cells is indicated. (**c**,**d**) Median fluorescence intensity (MFIs) were compared to the parental control vector (contr.). Transduction (Td) efficiencies: contr. GFP (83%, 78%), 5′ int. miRβ-GFP (66%, 68%), 5′ ex. miRβ-GFP (52%, 45%), 3′ ex. miRβ-GFP (62%, 63%). (**e**) GFP-encoding MP71 vectors expressing either each miRNA for the silencing of the TCR α (miRα) and β chain (miRβ) separately or both miRNAs together (miR). (**f**,**g**) TCR/CD3 complex surface levels and GFP expression were determined and compared to the parental vector (contr.). Td efficiencies: contr. (68%, 62%); miR-GFP (44%, 37%); miRα-GFP (51%, 50%); miRβ-GFP (47%, 42%). Plots show the mean of two independent experiments ± SD ($n = 2$).

RNAi-assisted TCR replacement results in equal surface levels of the transferred TCR chains

To analyze how TCR silencing and TCR gene optimization influence the expression of the P14 TCR, we introduced a second disulfide bond into the C regions of a codon-optimized P14 TCR cassette and generated the vectors P14opt and miR-P14opt. For analysis of the TCR-α and -β chain levels relative to each other, we compared transduced cells with nontransduced cells expressing endogenously the Vα2 and Vβ8 chains at a stoichiometry of 1:1. Although we transduced T cells with similar efficiencies using supernatants equilibrated in virus titer (**Supplementary Figure S3**), the P14 TCR-α and -β chain levels differed markedly between the samples (**Figure 3a**,**b**). Compared to the endogenous TCR expression, the P14 vector-transduced cells showed reduced and disparate TCR-α and -β chain levels of 24 and 64%. Notably, silencing of endogenous TCRs strongly reduced the difference between both TCR chain levels. For example, the TCR-α chain level increased from 24 to 36%, whereas the TCR-β chain level decreased from 64 to 42% if the miR cassette was coexpressed with the P14 TCR. This adjustment of the median fluorescence intensity (MFI) values was a unique effect of TCR silencing, because TCR gene optimization as employed in the P14opt vector did not change the difference between the MFI values similarly, but instead raised them individually to 46 and 78% for the TCR-α and -β chain, respectively.

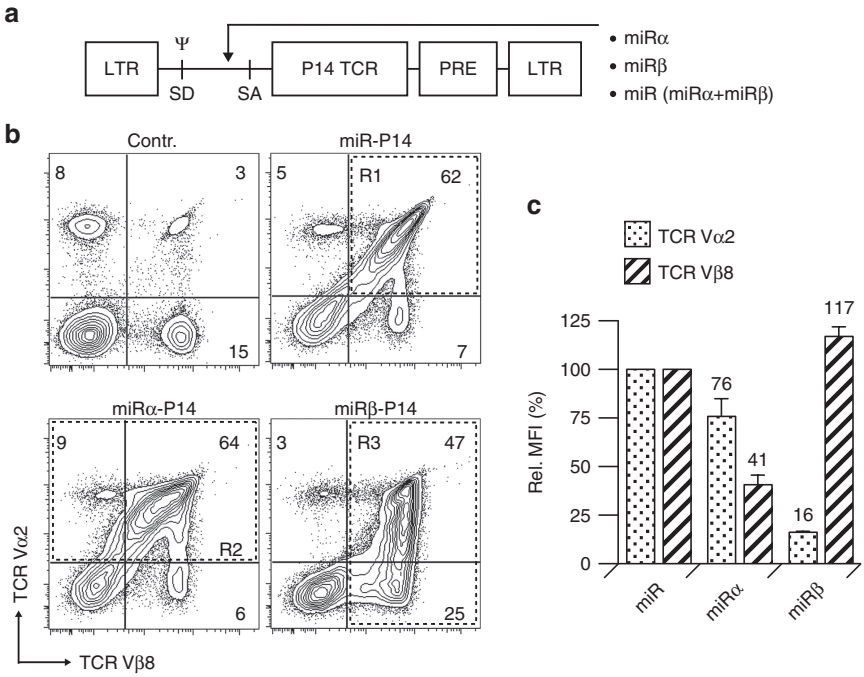

Figure 2 Silencing of the endogenous T cell receptor (TCR) supports the expression of an RNAi-resistant second TCR. (**a**) The miRNA vectors were used for the expression of an RNAi-resistant P14 TCR cassette. (**b**) The P14 TCR-α chain (TCR Vα2) and the P14 TCR-β chain (TCR Vβ8) surface levels of transduced polyclonal T cells were analyzed by flow cytometry. CD8 T cells are shown. Numbers indicate the percentage of cells in each the quadrant gate. Nontransduced T cells served as control (contr.). MFIs of the transduced cells were calculated using the gates R1 (miR-P14), R2 (miRα-P14), and R3 (miRβ-P14). (**c**) MFIs of cells expressing only one miRNA were compared to cells expressing both miRNAs. Transduction efficiencies: miR-P14 (62%, 62%); miRα-P14 (73%, 65%); miRβ-P14 (72%, 70%). Plot shows the mean of two independent experiments ± SD (n = 2).

Overall, the expression of the transferred TCR chains on miR-P14opt vector-transduced cells (TCR-α chain 81%, TCR-β chain 86%) resembled most the endogenous TCR expression. Likewise, this sample showed the highest percentage of Db-GP33-positive cells with the highest MFI (**Figure 3c,d**). However, TCR gene optimization improved the MHC multimer binding more effectively than TCR silencing. In particular, the ratio of P14 TCR expressing cells to Db-GP33-positive cells was improved from 0.41 to 0.50 if the miR cassette was coexpressed with the P14 TCR, but optimization of the P14 TCR improved this ratio to 0.65. Furthermore, compared to P14 vector-transduced cells the Db-GP33 MFI was 1.14-fold improved by TCR silencing and 1.65-fold by TCR gene optimization. These data reveal that silencing the endogenous TCR and TCR gene optimization affected the P14 TCR-α and -β chain levels in different ways. The amount of P14 TCR was improved to a greater extent by TCR gene optimization but, in contrast to TCR silencing, this technique did not result in equal P14 TCR-α and -β chain levels, which implies that the amount of mixed TCR dimers was not concomitantly reduced.

miR-TCR gene-modified T cells show antitumor reactivity and increased antigen-specific proliferation

Having studied the specific RNAi effect, we next analyzed if the expression of the RNAi-resistant P14 TCR resulted in a functional reconstitution of the T cells with silenced endogenous TCR. Hypothetically, the expression of the miRNA cassette could induce off-target effects, either in a sequence specific manner[35] or by saturation of the endogenous miRNA pathway,[36] resulting in impaired cell survival, proliferation and effector function. Therefore, we compared transduced T cells expressing the native or optimized P14 TCR genes with and without silenced endogenous TCR in a tumor suppression model. We treated mice that were injected with GP33-expressing B16.F10 melanoma cells with transduced T cells and analyzed the engraftment and expansion of the transferred cells, as well as suppression of tumor growth. Enhanced on-target effects due to differences in the P14 TCR surface levels, however, might not be observable, as it was demonstrated that even P14 TCR-transgenic T cells were hardly more effective than P14 vector-transduced T cells in this model.[37] Indeed, comparable suppression of tumor growth was achieved irrespective of the particular vector used for transduction as no significant differences in the number of pulmonary metastasis among the treatment groups were observed (**Figure 4a,b** and **Supplementary Figure S5a**). The average number of metastases was 27 for the P14 group and 25 for the P14opt group, showing that the increase of the P14 TCR level by TCR gene optimization did not significantly alter the outcome. No negative effects of the miR cassette were detected either, as on average 30 and 22 metastasis were found in the groups that received T cells expressing the miR cassette and either the native or optimized P14 TCR. Successful engraftment, proliferation, and stable TCR expression was confirmed by analyzing peripheral blood samples. Regardless of whether the miR cassette was expressed together with the native or optimized P14 TCR, the percentage and MFI of Db-GP33-positive cells were significantly increased (**Figure 4c,d** and **Supplementary Figure S5b**). After 1 week, on average 36 and 55% of the transferred CD8-positive T cells were stained by the Db-GP33 multimer in the P14 group and the P14opt group, whereas 59 and 83% Db-GP33-positive cells were detected in the miR-P14 group and

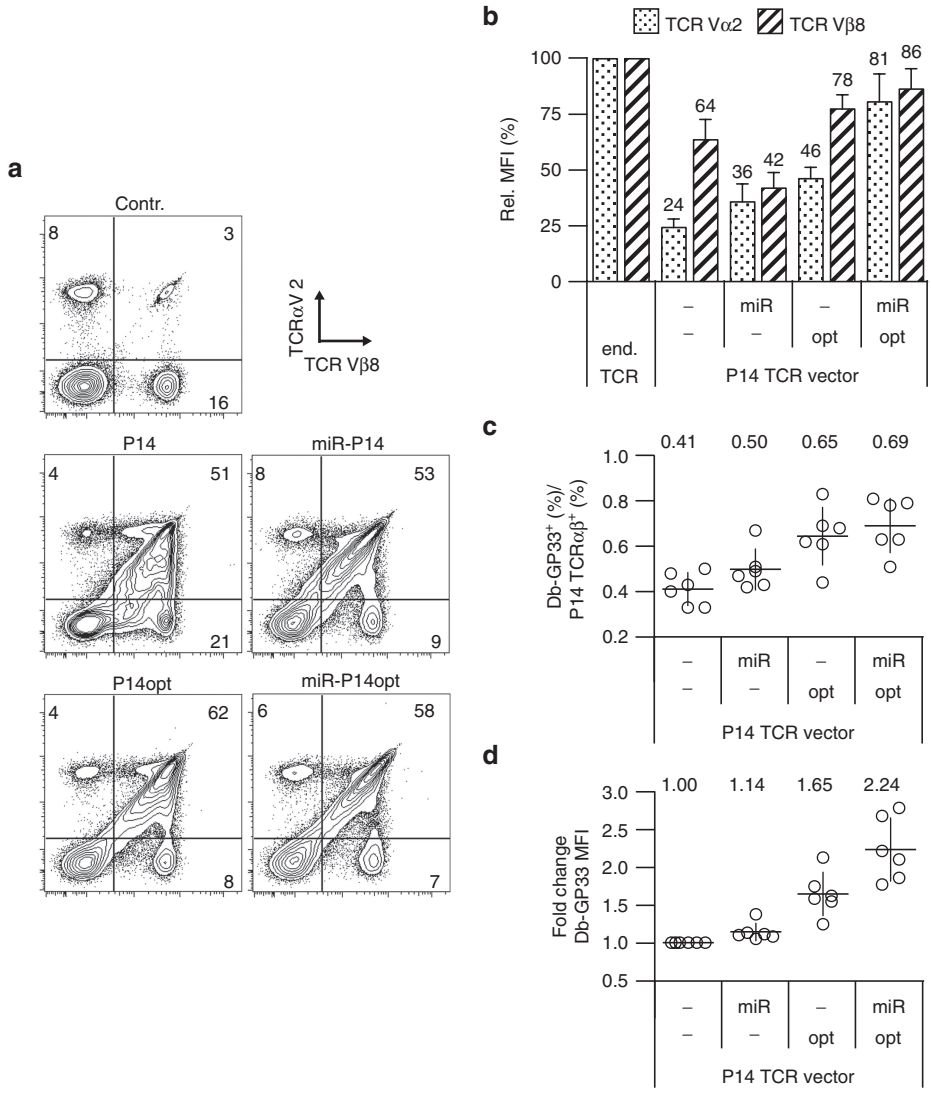

Figure 3 RNAi-assisted T cell receptor (TCR) replacement results in equal surface levels of the transferred TCR chains. (**a**) Polyclonal T cells were transduced with four P14 TCR vectors differing from each other by the presence of the intronic miR cassette (miR) and the usage of the optimized P14 TCR cassette (opt). Cells were stained either for CD8 and for both P14 TCR chains (TCR Vα2, TCR Vβ8) or for CD8 and using a P14 TCR-specific MHC multimer (Db-GP33). CD8 T cells are shown and the percentages of the gated cells are indicated. Nontransduced T cells served as control (contr.). (**b**) Median fluorescence intensity (MFIs) of transduced CD8 T cells were compared to nontransduced CD8/Vα2Vβ8 T cells (end. TCR). (**c**) Plot shows the proportion of cells expressing both P14 TCR chains that bind the Db-GP33 multimer. (**d**) Plot shows the fold change of the Db-GP33 multimer MFI relative to the P14 vector-transduced sample. Horizontal bar (group mean, indicated on top). Vertical bar (SD). Combined data of six independent experiments are shown in **b**, **c**, and **d** ($n = 6$). Transduction efficiencies were comparable (**Supplementary Figure S3b**).

the miR-P14opt group. In addition to these results, we found no differences in proliferation, INF-γ production or peptide sensitivity in *in vitro* experiments comparing T cells transduced with control and miRNA vectors (**Supplementary Figure S4**). These data provide no evidence for RNAi-related off-target effects. Our results also indicate that the increased amount of P14 TCR leads to enhanced antigen-driven proliferation of the T cells expressing either the miR cassette or the optimized P14 TCR, with the highest level of proliferation being seen with the combination of both.

RNAi-assisted TCR replacement severely reduces TI-GVHD caused by mixed TCR dimers

To analyze the effect of RNAi-assisted TCR replacement on the formation of self-reactive mixed TCR dimers, we took advantage of a mouse model in which mixed TCR dimers induce TI-GVHD.[13] In this model, the clinical protocol of TCR gene therapy is mimicked and unsorted TCR-transduced T cells were transferred into irradiated mice that were treated afterwards with IL-2. We hypothesized that the P14 TCR would cause a high incidence of TI-GVHD, because expression of the P14 TCR-α and -β chain at the surface of transduced T cells is highly unequal even when using a TCR cassette with a 2A element (**Figure 3b**). Indeed, all mice that received transduced T cells expressing the native P14 TCR developed lethal TI-GVHD within 30 days, whereas no autoimmunity was induced after transfer of P14 TCR-transgenic T cells or nontransduced T cells (control) (**Figure 5a**). The observed symptoms and kinetics were similar to those described for other TCRs in this model, including the rapid weight loss (**Figure 5b**). The

disappearance of hematopoietic cells in the bone marrow and the massive reduction of the periarteriolar lymphatic sheaths in the spleen, two characteristic manifestations of TI-GVHD, were confirmed in recipients of P14 vector-transduced T cells. The same organs from recipients of P14 TCR-transgenic or nontransduced T cells did not show pathologic changes (**Supplementary Figure S6**). Notably, P14 TCR-transduced T cells induced the highest incidence of TI-GVHD compared to T cells modified with other TCRs.[13] Next, we investigated whether the usage of codon-optimized TCR genes which additionally harbor a second disulfide bond or the silencing of the endogenous TCR chains by miRNAs can prevent TI-GVHD. All mice that received transduced T cells expressing the native or the optimized P14 TCR developed lethal TI-GVHD (**Figure 5c**). In contrast, despite the unprecedented high incidence of TI-GVHD observed following gene transfer with the native P14 TCR, only three out of 16 mice that received P14 TCR-transduced T cells with silenced endogenous TCR developed TI-GVHD. Moreover, when RNAi-mediated knockdown of the endogenous TCR was combined with the expression of the optimized P14 TCR genes, only one mouse out of 16 developed TI-GVHD (**Figure 5c**). The body weights of the two groups that were treated with T cells just expressing the native or optimized P14 TCR differed significantly from those two groups that were treated with T cells expressing the same TCRs but in addition also the miR cassette (**Figure 5d**). Analysis of peripheral blood confirmed engraftment and expansion of transduced T cells. These data indicate that in case of the P14 TCR only the silencing of the endogenous TCR and not the use of optimized TCR genes efficiently reduces the amount of mixed TCR dimers on TCR-transduced T cells and the incidence of lethal TI-GVHD in mice receiving these cells.

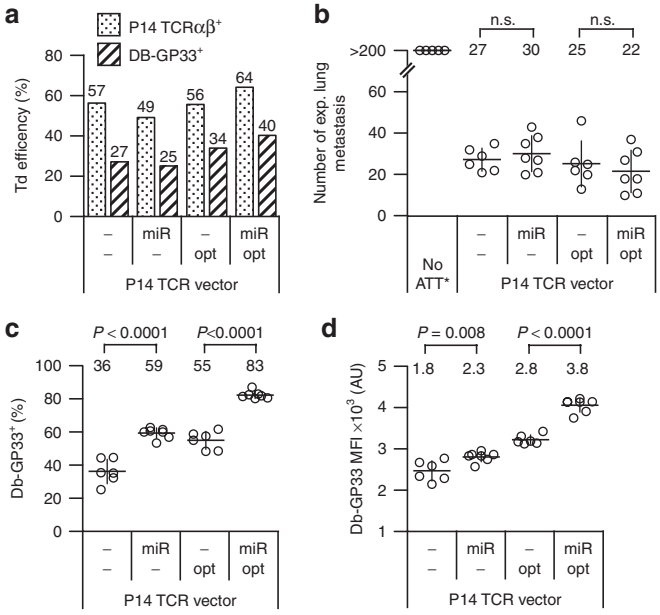

Figure 4 miR-T cell receptor (TCR) gene-modified T cells show antitumor reactivity and increased antigen-specific proliferation. (**a**) Transduced polyclonal T cells were analyzed either for the expression of both P14 TCR chains (P14 TCRαβ) or binding of the P14 TCR-specific MHC multimer (Db-GP33) at the day of adoptive T cell transfer (ATT). 2×10^6 congenic CD8/P14 TCRαβ T cells (B6.SJL) were transferred into recipients (C57BL/6) that received 3 days before 1×10^6 GP33-expressing tumor cells (B16-GP33) intravenously. (**b**) Plot shows the number of macroscopically visible experimental (exp.) lung metastasis 21 days after ATT. *The mice of the control group without ATT were sacrificed after 14 days. (**c**,**d**) Transferred T cells in peripheral blood were analyzed at day 7 after ATT. Results were confirmed by a second measurement at day 14 (**Supplementary Figure S5**). Symbols represent individual mice. Horizontal bar (group mean, indicated on top). Vertical bar (SD). Group sizes: P14 ($n = 6$), miR-P14 ($n = 7$), P14opt ($n = 6$), miR-P14opt ($n = 7$), control ($n = 5$).

DISCUSSION

In this study, we demonstrate in an *in vivo* model of TCR gene therapy that RNAi-mediated silencing of the endogenous TCR minimizes the expression of mixed TCR dimers on TCR gene-modified T cells and severely reduces the risk of autoimmunity. Previously, it has been shown, that an additional disulfide bond in the TCR C regions and the linkage of both TCR chains by a 2A element avoided TI-GVHD in case of one TCR and greatly diminished TI-GVHD in case of another TCR.[13] Here we provide evidence, that these measures were not sufficient for TCRs such as the P14 TCR for which mixed TCR dimer formation is pronounced (**Figure 5**). The unequal surface levels of the P14 TCR-α and -β chain on transduced T cells indicate that they possess different abilities to compete with the endogenous TCR chains for surface expression (**Figure 3**). This difference between the two P14 TCR chains remained dominant even after the TCR genes were codon-optimized and an additional disulfide bond was introduced. Silencing of the endogenous TCR on the contrary mitigated the TCR competition and resulted in equal surface expression levels of both P14 TCR chains.

In case of the P14 TCR, the measurement of the surface levels of both TCR chains has proven to be a more useful indicator for the amount of mixed TCR dimers compared to either MHC multimer staining or the calculation of the ratio of T cells binding the MHC multimer to T cells expressing the P14 TCR chains (**Figure 3**). The reason is that the amount of correctly paired P14 TCR per cell might reflect either a higher percentage of correctly paired TCR chains or the expression of more correctly paired TCR chains without a change of the ratio of correctly paired TCR chains to mixed TCR dimers. Therefore, the determination of the TCR chain surface levels might serve to identify TCRs that are prone to induce autoimmunity. Although the notion that unequal surface levels indicate the formation of mixed TCR dimers has already been made,[2] the prevalence of this phenomenon among the TCRs that were either suggested for or have already been used in clinical trials of TCR gene therapy is currently unknown.

Our study provides a direct link between unequal TCR chain surface levels after the transfer of both TCR genes and the development of TI-GVHD. We show that all mice in those two groups developed fatal TI-GVHD that received TCR gene-modified T cells with unequal TCR-α and -β chain surface levels, whereas 86% of the animals survived in both groups that received TCR gene-modified T cells expressing the transferred TCR chains but at equal levels (**Figure 5**).

Initially, RNAi-mediated protein replacement was used to study RNAi-related off-target effects.[38,39] It was then suggested for the treatment of hereditary diseases[40] and later for improving the expression of the transferred TCR in TCR gene therapy.[19]

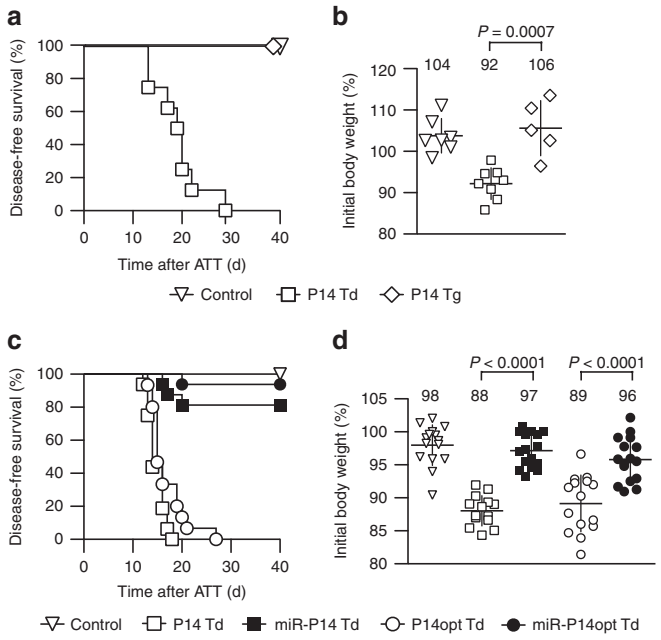

Figure 5 RNAi-assisted T cell receptor (TCR) protein replacement severely reduces the incidence of TI-GVHD caused by mixed TCR dimers. (**a**,**b**) TI-GVHD is induced by P14 vector-transduced (Td) T cells but not by P14 TCR-transgenic (Tg) T cells. Cell populations containing 1×10^6 P14 TCR-expressing CD8 cells were transferred into irradiated mice. Ten days after adoptive T cell transfer (ATT), the mice were treated for 3 days with IL-2 twice a day and monitored for autoimmune symptoms. The control group was treated identical but received non-transduced T cells. A Kaplan–Meier plot of disease-free survival and the change of body weight at day 14 after ATT are shown in **a** and **b**, respectively. Horizontal bar (group mean, indicated on top). Vertical bar (SD). Group sizes, Td efficiencies: control ($n = 7$), P14 Td ($n = 8$, 20%), P14 Tg ($n = 5$). (**c**,**d**) TI-GVHD is reduced in mice receiving P14 TCR-transduced T cells with silenced endogenous TCR. Results of two independent experiments are shown in **c** (Kaplan–Meier plot) and **d** (change of body weight at day 12 after ATT). Two mice of the P14 group had to be sacrificed because of TI-GVHD at day 11 and were therefore not included in **d**. Horizontal bar (group mean, indicated on top). Vertical bar (SD). Group sizes, Td efficiencies: control ($n = 15$), P14 ($n = 16$, 55%, 56%), miR-P14 ($n = 16$, 35%, 62%), P14opt ($n = 15$, 44%, 21%), miR-P14opt ($n = 16$, 65%, 57%).

Recently, two studies addressed how to design an RNAi-assisted TCR replacement vector for human T cells.[27,29] The silencing of the human TCR has been analyzed mainly on the mRNA level using bulk preparations or indirectly by staining the transferred RNAi-resistant TCR with an MHC multimer. From such data, it is difficult to conclude on the remaining amount of endogenous TCR protein in the whole population of transduced T cells. We used vectors expressing GFP and miRNA to quantify the TCR silencing on the protein level with single-cell resolution. The silencing efficiency was strictly proportional to the GFP expression and varied within the population of transduced T cells (**Figure 1**). Differences in the vector copy number and vector integration sites within the cell population could explain this observation. Possibly, residual endogenous TCR protein in some of the cells might be responsible for the few cases of TI-GVHD observed after the transfer of T cells transduced with the RNAi-TCR replacement vector. A closer investigation of the autoreactive T cells would be necessary to confirm this hypothesis. We cannot formally exclude, however, that the silencing efficiency in the autoreactive T cells could have been affected due to other reasons.

Besides the silencing efficiency, high transduction rates and a strong expression of the therapeutic TCR are desirable to replace as much as possible of remaining endogenous TCR. Indeed, the usage of optimized TCR genes in the RNAi-TCR replacement vector improved the P14 TCR level and resulted in a somewhat lower incidence of TI-GVHD (**Figures 3** and **5**). TCR gene optimization likely partially alleviates the negative effect of the introduced miRNA on the transgene expression level of the vector. Our data demonstrate, that a vector design that generates mRNAs encoding miRNA and protein results in decreased protein levels, because the processing of the miRNA produces truncated mRNAs. This is in accordance with previously published data.[31,41] Intronic miRNA has the potential to resolve this issue, as the splicing mechanism can religate the mRNA after the miRNA has been excised (**Figure 1**). It is therefore plausible, that the usage of a more efficient intron would further improve the transgene expression. The MP71 intron, however, also contains the packaging signal (ψ) and this configuration ensures that only transcripts containing the unspliced intron are packaged into virions. Improving the splicing efficiency might therefore influence the viral titer, which was hardly affected by the introduced miRNAs in this study (**Supplementary Figure S3a**).

The description of mixed TCR dimer-induced autoimmunity in mice and the detection of autoreactive mixed TCR dimers on transduced human T cells in *in vitro* assays have stimulated a reexamination of clinical data from past TCR gene therapy studies.[42] No signs of off-target toxicities caused by mixed TCR dimers were detected in humans so far, whereas TI-GVHD in the mouse model was observed in different degrees with every TCR tested. It is clear, though, that the initial studies in human resulted in mixed therapeutic success and that the clinical protocol of TCR gene therapy is still under development. In mouse models, mixed TCR dimer-dependent autoimmunity was not seen until specific conditions were established. Intriguingly, these conditions resemble the clinical situation with regard to the lymphodepleting pretreatment of the host and the IL-2 treatment after T cell transfer. Whether particular differences between mice and men exist that exclude TI-GVHD in future TCR gene therapy trials employing new TCRs and improved protocols can only be speculated.

In this study, we were able to almost completely avoid TI-GVHD using a combination of RNAi-mediated knockdown of the endogenous TCR and genetically optimized TCR genes. Only one out of 16 mice developed TI-GVHD despite an incidence of 100% if optimized TCR genes were applied without endogenous TCR silencing (**Figure 5**). Our data support the usage of RNAi for the generation of human TCR gene-modified T cells and the broader range of vector systems available for human T cells might also allow the development of improved RNAi-based TCR replacement vectors. We provided evidence that silencing of the endogenous TCR has the unique advantage of mitigating the TCR competition in TCR gene-modified T cells and that safe application of TCRs that are prone to form mixed TCR dimers in adoptive T cell therapy requires such measures.

MATERIALS AND METHODS

Mice. C57BL/6 and B6.SJL mice (CD45.1$^+$) were purchased from Charles River (Sulzfeld, Germany). Transgenic mice, expressing either the H2-Db-restricted TCR I (Vα3, Vβ7) specific for the simian virus 40 large tumor antigen epitope I (SV40I)[34] or the H2-Db-restricted P14 TCR (Vα2, Vβ8) specific for the LMCV GP33-41 epitope[33] were purchased from The Jackson Laboratory (Sulzfeld, Germany). All animal experiments were conducted in accordance with institutional and national guidelines, after approval by a state animal ethics committee (Landesamt für Gesundheit und Soziales, Berlin).

Construction of retroviral vectors. The miRNAs that were introduced into the MP71-GFP vector[17] were generated by overlap polymerase chain reaction (PCR) (**Supplementary Figure S1a,b**). The miR-155 template[31] (165bp) was amplified from genomic mouse DNA and the template for the artificial miRNA[32] (172bp) was synthesized. RNAi target sites were identified using web-based software.[43,44] The following antisense sequences were chosen for the silencing of the endogenous mouse TCR chains: 5′-TTTAGGTTCATATCTGTTTCA-3′ (TCR α) and 5′-CTGATGTTCTGTGTGACAGGT-3′ (TCR β). miRNA-TCR vectors were generated by the exchange of GFP for the P14 TCR cassette.[45] P14 TCR (Vα2, Vβ8) is specific for the LMCV-derived epitope GP33-41 presented by H-2Db.[33] The native P14 TCR genes were rendered RNAi-resistant by partial codon optimization (**Supplementary Figure S1c**). Fully codon-optimized P14 TCR genes were additionally modified by a threonine into cysteine exchange at the position 187 in the TCR α chain and a serine into cysteine exchange at the position 199 in the TCR β chain.

Retroviral transduction and culture of mouse T cells. Ecotropic retrovirus particles were produced using the Platinum-E packaging cell line.[46] Supernatants were harvested 48 hours after transfection, filtrated (0.45 µm pore size) and frozen (−80 °C). Mouse splenocytes were transduced using diluted supernatants to determine the concentration that results in a transduction rate of 50% (**Supplementary Figure S3a**). Nontransduced control cells were always prepared in parallel with the transduced cells and subjected to the same protocol except that the packaging cells were not transfected with vector DNA. Mouse splenocytes were subjected to two rounds of transduction. 0.5 ml/well supernatant was transferred to a RetroNectin-coated (Takara, Saint-Germain-en-Laye, France) 24-well nontissue culture plate, centrifuged (3,000 *g*, 4 °C) for 3 hours and immediately discharged before the activated splenocytes were transferred into the plates. Afterwards, the splenocytes were centrifuged (800 *g*, 32 °C) for 20 minutes and cultured over night. Then, 1 ml/well viral supernatant supplemented with 10 IU Proleukin (Novartis, Nuremberg, Germany) and 4 µg protamine sulfate (Sigma-Aldrich, Taufkirchen, Germany) was added and the cells were centrifuged (800 *g*, 32 °C) for 1.5 hours. Splenocytes were isolated 1 day before the transduction, adjusted to 2×10^6 cells/ml and activated for 24 hours with 1 µg/ml anti-CD3 mAb, 0.1 µg/ml anti-CD28 mAb (both BD Biosciences, Heidelberg, Germany) and 10 IU/ml Proleukin. For the first transduction, the culture medium was exchanged, the cell density was adjusted to 1×10^6 cells/ml and 4×10^5 beads/ml mouse T-Activator CD3/CD28 (Life Technologies, Karlsruhe, Germany), 10 IU/ml Proleukin and 4 µg/ml protamine sulfate were added. Then 1×10^6 cells/well were transferred onto the virus-coated plates. After the transduction, the cells were washed and adjusted to 1×10^6 cells/ml in medium supplemented with 10 ng/ml human recombinant IL-15 (Peprotech, Hamburg, Germany). This step was repeated every 3–4 days during prolonged culture of the transduced splenocytes.

Melanoma lung metastases model. The GP33-expressing melanoma cell line (B16-GP33)[47] was cultured under G418 selection (1 mg/ml) (Life Technologies). Tumor cells were split one day before 1×10^6 B16-GP33 cells per mice (C57BL/6) were injected into the tail vein. Three days later 2×10^6 P14 TCR-expressing CD8$^+$ T cells (B6.SJL) per mice were injected similarly. Seven days and 14 days after T cell transfer, blood samples were analyzed. After 2 weeks, tumor growth was inspected and the mice of the control group were sacrificed. The mice of the treatment groups were sacrificed after 21 days and the number of macroscopically visible metastases on the lung surface was counted.

TI-GVHD model. The TI-GVHD model was carried out as previously described.[13] Retroviral particles were generated using the Phoenix Ecotropic packaging cell line. Mouse splenocytes were activated for 48 hours by concovalin A (2 µg/ml, Sigma-Aldrich) and IL-7 (1 ng/ml, Peprotech) before they were subjected to one round of transduction. Activated splenocytes were resuspended in viral supernatant and transferred into RetroNectin-coated 24-well nontissue culture plates, centrifuged (800 *g*, 23 °C) for 1.5 hours and incubated over night. The transduction rate was determined by flow cytometry and an unsorted population of cells containing 1×10^6 P14 TCR-expressing CD8 T cells was transferred into mice (C57BL/6) that were treated 1 day before with total body irradiation (TBI, 5 Gy). Ten days after ATT, the mice received 7.2×10^5 IU Proleukin (Novartis) intraperitoneally twice a day for 3 days and were monitored thoroughly (weight, appearance, behavior). Group assignments were blinded.

Histological analysis. Spleen and bone marrow (femur) of mice were collected and fixed with 4% buffered paraformaldehyde. Bones were decalcified using ethylenediaminetetraacetic acid. Paraffin-embedded tissues were cut in sections (3 µm thickness), dried (70 °C, 30 minutes), deparaffinized in xylene and dehydrated through graded alcohols. Sections were stained using hematoxylin and eosin (H&E) and analyzed using a bright-field microscope (BX53, Olympus, Hamburg, Germany) equipped with a digital camera (DP25, Olympus).

Flow cytometry. If not stated otherwise, flow cytometry data were acquired 4–6 days after transduction. Relative MFIs values were calculated by dividing the MFIs of the samples by the MFI of the control sample as specified in the figure legend. TCR surface levels of GFP-expressing T cells were determined using allophycocyanin (APC)-labeled anti-mouse TCR Cβ region mAb (H57-597, BioLegend, London, UK) or APC-labeled anti-mouse CD3ε mAb (145-2C11, BioLegend). P14 TCR chain expression was analyzed using fluorescein isothiocyanate (FITC)-labeled anti-mouse TCR Vβ8 mAb (MR5-2, BioLegend), phycoerythrin (PE)-labeled anti-mouse CD8α mAb (53-6.7, BioLegend) and APC-labeled anti-mouse TCR Vα2 mAb (B20.1, BioLegend). TCR-transgenic T cells were stained with PE-labeled H2-Db SAINNYAQKL (Db-SV40I) multimer and APC-labeled H2-Db KAVYNFATC (Db-GP33) multimer (both iTAG, Beckman Coulter, Krefeld, Germany). P14 TCR chain pairing was analyzed using PE-labeled anti-mouse CD8α mAb and APC-labeled Db-GP33 multimer. Adoptively transferred T cells were analyzed by staining the peripheral blood samples with unlabeled anti-mouse CD16/CD32 mAb (2.4G2, BD Bioscience), FITC-labeled anti-mouse CD8α mAb (53-6.7, BioLegend), PE-labeled anti-mouse CD45.1 mAb (A20, BioLegend) and Db-GP33 multimer. Cells were stained in buffer (phosphate-buffered saline, 2 mmol/l ethylenediaminetetraacetic acid, 2% fetal calf serum, 0.05% NaN_3) for 30 minutes at 4 °C in the dark, washed twice and resuspended in buffer containing SYTOX Blue (Life Technologies). Immunofluorescence was measured using a FACS Canto II cytometer (BD Biosciences) or a MACS Quant Analyzer (Miltenyi Biotec, Bergisch Gladbach, Germany). Data were analyzed using FlowJo software (Tree Star, Ashland, OR).

Cytokine secretion assay. 5×10^4 CD8$^+$/P14 TCR$^+$ T cells were cocultured for 24 hours with 5×10^4 syngeneic mouse splenocytes preloaded with peptide and the INF-γ concentration in the supernatant was determined by enzyme-linked immunosorbent assay (BD Bioscience). The HPLC-purified GP33 peptide (KAVYNFATM) was purchased from Biosynthan (Berlin, Germany).

Statistical analysis. The unpaired two-tailed Student's *t*-test was used to calculate the indicated *P* values with the software Prism (GraphPad, La Jolla, CA).

SUPPLEMENTARY MATERIAL

Figure S1. Molecular construction of the miRNA vectors for TCR silencing.

Figure S2. TCR I-transgenic T cells transduced with the miR-P14 vector lose their ability to bind TCR I-specific MHC multimers.

Figure S3. Viral supernatants were titrated to achieve comparable transduction efficiencies.

Figure S4. No miRNA off-target effects were detected in in vitro assays testing antigen-stimulated cytokine production and proliferative capacity.

Figure S5. Suppression of experimental pulmonary metastasis and antigen-driven proliferation.

Figure S6. Disappearance of hematopoietic cells in the bone marrow and reduction of lymphocytes in the spleen caused by TI-GVHD.

ACKNOWLEDGMENTS

We thank S Reuss (MDC, Berlin) for providing the P14opt vector, T Blankenstein (MDC, Berlin) for helpful discussions and C Genehr (MDC, Berlin), M Richter (MDC, Berlin), and N Gatzemeier (CCM, Berlin) for technical assistance. This work was supported by grants from the Deutsche Forschungsgemeinschaft (SFB-TR 36 to W.U.). Contribution statement: M.B. developed the RNAi vector and performed *in vitro* experiments; M.B., G.B., C.L., and L.B. performed *in vivo* experiments; S.S. performed histological analysis; T.N.S. and W.U. supervised the research, contributed experimental design and data interpretation; M.B. wrote the manuscript. G.B., C.L., T.N.S., and W.U. reviewed and edited the manuscript. The authors declare no conflict of interest.

REFERENCES

1. Clay, TM, Custer, MC, Sachs, J, Hwu, P, Rosenberg, SA and Nishimura, MI (1999). Efficient transfer of a tumor antigen-reactive TCR to human peripheral blood lymphocytes confers anti-tumor reactivity. *J Immunol* **163**: 507–513.
2. Cooper, LJ, Kalos, M, Lewinsohn, DA, Riddell, SR and Greenberg, PD (2000). Transfer of specificity for human immunodeficiency virus type 1 into primary human T lymphocytes by introduction of T-cell receptor genes. *J Virol* **74**: 8207–8212.
3. Fujio, K, Misaki, Y, Setoguchi, K, Morita, S, Kawahata, K, Kato, I *et al.* (2000). Functional reconstitution of class II MHC-restricted T cell immunity mediated by retroviral transfer of the alpha beta TCR complex. *J Immunol* **165**: 528–532.
4. Kessels, HW, Wolkers, MC, van den Boom, MD, van der Valk, MA and Schumacher, TN (2001). Immunotherapy through TCR gene transfer. *Nat Immunol* **2**: 957–961.
5. de Witte, MA, Coccoris, M, Wolkers, MC, van den Boom, MD, Mesman, EM, Song, JY *et al.* (2006). Targeting self-antigens through allogeneic TCR gene transfer. *Blood* **108**: 870–877.
6. Morgan, RA, Dudley, ME, Wunderlich, JR, Hughes, MS, Yang, JC, Sherry, RM *et al.* (2006). Cancer regression in patients after transfer of genetically engineered lymphocytes. *Science* **314**: 126–129.
7. Johnson, LA, Morgan, RA, Dudley, ME, Cassard, L, Yang, JC, Hughes, MS *et al.* (2009). Gene therapy with human and mouse T-cell receptors mediates cancer regression and targets normal tissues expressing cognate antigen. *Blood* **114**: 535–546.
8. Robbins, PF, Morgan, RA, Feldman, SA, Yang, JC, Sherry, RM, Dudley, ME *et al.* (2011). Tumor regression in patients with metastatic synovial cell sarcoma and melanoma using genetically engineered lymphocytes reactive with NY-ESO-1. *J Clin Oncol* **29**: 917–924.
9. Parkhurst, MR, Yang, JC, Langan, RC, Dudley, ME, Nathan, DA, Feldman, SA *et al.* (2011). T cells targeting carcinoembryonic antigen can mediate regression of metastatic colorectal cancer but induce severe transient colitis. *Mol Ther* **19**: 620–626.
10. Morgan, RA, Chinnasamy, N, Abate-Daga, D, Gros, A, Robbins, PF, Zheng, Z *et al.* (2013). Cancer regression and neurological toxicity following anti-MAGE-A3 TCR gene therapy. *J Immunother* **36**: 133–151.
11. Schumacher, TN (2002). T-cell-receptor gene therapy. *Nat Rev Immunol* **2**: 512–519.
12. van Loenen, MM, de Boer, R, Amir, AL, Hagedoorn, RS, Volbeda, GL, Willemze, R *et al.* (2010). Mixed T cell receptor dimers harbor potentially harmful neoreactivity. *Proc Natl Acad Sci USA* **107**: 10972–10977.
13. Bendle, GM, Linnemann, C, Hooijkaas, AI, Bies, L, de Witte, MA, Jorritsma, A *et al.* (2010). Lethal graft-versus-host disease in mouse models of T cell receptor gene therapy. *Nat Med* **16**: 565–70, 1p following 570.
14. Saito, T, Sussman, JL, Ashwell, JD and Germain, RN (1989). Marked differences in the efficiency of expression of distinct alpha beta T cell receptor heterodimers. *J Immunol* **143**: 3379–3384.
15. Sommermeyer, D, Neudorfer, J, Weinhold, M, Leisegang, M, Engels, B, Noessner, E *et al.* (2006). Designer T cells by T cell receptor replacement. *Eur J Immunol* **36**: 3052–3059.
16. Heemskerk, MH, Hagedoorn, RS, van der Hoorn, MA, van der Veken, LT, Hoogeboom, M, Kester, MG *et al.* (2007). Efficiency of T-cell receptor expression in dual-specific T cells is controlled by the intrinsic qualities of the TCR chains within the TCR-CD3 complex. *Blood* **109**: 235–243.
17. Engels, B, Cam, H, Schüler, T, Indraccolo, S, Gladow, M, Baum, C *et al.* (2003). Retroviral vectors for high-level transgene expression in T lymphocytes. *Hum Gene Ther* **14**: 1155–1168.
18. Szymczak, AL, Workman, CJ, Wang, Y, Vignali, KM, Dilioglou, S, Vanin, EF *et al.* (2004). Correction of multi-gene deficiency *in vivo* using a single 'self-cleaving' 2A peptide-based retroviral vector. *Nat Biotechnol* **22**: 589–594.
19. Scholten, KB, Kramer, D, Kueter, EW, Graf, M, Schoedl, T, Meijer, CJ *et al.* (2006). Codon modification of T cell receptors allows enhanced functional expression in transgenic human T cells. *Clin Immunol* **119**: 135–145.
20. Cohen, CJ, Zhao, Y, Zheng, Z, Rosenberg, SA and Morgan, RA (2006). Enhanced antitumor activity of murine-human hybrid T-cell receptor (TCR) in human lymphocytes is associated with improved pairing and TCR/CD3 stability. *Cancer Res* **66**: 8878–8886.
21. Voss, RH, Kuball, J, Engel, R, Guillaume, P, Romero, P, Huber, C *et al.* (2006). Redirection of T cells by delivering a transgenic mouse-derived MDM2 tumor antigen-specific TCR and its humanized derivative is governed by the CD8 coreceptor and affects natural human TCR expression. *Immunol Res* **34**: 67–87.
22. Kuball, J, Dossett, ML, Wolfl, M, Ho, WY, Voss, RH, Fowler, C *et al.* (2007). Facilitating matched pairing and expression of TCR chains introduced into human T cells. *Blood* **109**: 2331–2338.
23. Cohen, CJ, Li, YF, El-Gamil, M, Robbins, PF, Rosenberg, SA and Morgan, RA (2007). Enhanced antitumor activity of T cells engineered to express T-cell receptors with a second disulfide bond. *Cancer Res* **67**: 3898–3903.
24. Sommermeyer, D and Uckert, W (2010). Minimal amino acid exchange in human TCR constant regions fosters improved function of TCR gene-modified T cells. *J Immunol* **184**: 6223–6231.
25. Bialer, G, Horovitz-Fried, M, Ya'acobi, S, Morgan, RA and Cohen, CJ (2010). Selected murine residues endow human TCR with enhanced tumor recognition. *J Immunol* **184**: 6232–6241.
26. Provasi, E, Genovese, P, Lombardo, A, Magnani, Z, Liu, PQ, Reik, A *et al.* (2012). Editing T cell specificity towards leukemia by zinc finger nucleases and lentiviral gene transfer. *Nat Med* **18**: 807–815.
27. Okamoto, S, Mineno, J, Ikeda, H, Fujiwara, H, Yasukawa, M, Shiku, H *et al.* (2009). Improved expression and reactivity of transduced tumor-specific TCRs in human lymphocytes by specific silencing of endogenous TCR. *Cancer Res* **69**: 9003–9011.
28. Ochi, T, Fujiwara, H, Okamoto, S, An, J, Nagai, K, Shirakata, T *et al.* (2011). Novel adoptive T-cell immunotherapy using a WT1-specific TCR vector encoding silencers for endogenous TCRs shows marked antileukemia reactivity and safety. *Blood* **118**: 1495–1503.
29. Okamoto, S, Amaishi, Y, Goto, Y, Ikeda, H, Fujiwara, H, Kuzushima, K *et al.* (2012). A Promising Vector for TCR Gene Therapy: Differential Effect of siRNA, 2A Peptide, and Disulfide Bond on the Introduced TCR Expression. *Mol Ther Nucleic Acids* **1**: e63.
30. Reuß, S, Sebestyén, Z, Heinz, N, Loew, R, Baum, C, Debets, R *et al.* (2014). TCR-engineered T cells: a model of inducible TCR expression to dissect the interrelationship between two TCRs. *Eur J Immunol* **44**: 265–274.
31. Chung, KH, Hart, CC, Al-Bassam, S, Avery, A, Taylor, J, Patel, PD *et al.* (2006). Polycistronic RNA polymerase II expression vectors for RNA interference based on BIC/miR-155. *Nucleic Acids Res* **34**: e53.
32. Saetrom, P, Snøve, O, Nedland, M, Grünfeld, TB, Lin, Y, Bass, MB *et al.* (2006). Conserved microRNA characteristics in mammals. *Oligonucleotides* **16**: 115–144.
33. Pircher, H, Michalopoulos, EE, Iwamoto, A, Ohashi, PS, Baenziger, J, Hengartner, H *et al.* (1987). Molecular analysis of the antigen receptor of virus-specific cytotoxic T cells and identification of a new V alpha family. *Eur J Immunol* **17**: 1843–1846.
34. Staveley-O'Carroll, K, Schell, TD, Jimenez, M, Mylin, LM, Tevethia, MJ, Schoenberger, SP *et al.* (2003). *In vivo* ligation of CD40 enhances priming against the endogenous tumor antigen and promotes CD8+ T cell effector function in SV40 T antigen transgenic mice. *J Immunol* **171**: 697–707.
35. Jackson, AL, Bartz, SR, Schelter, J, Kobayashi, SV, Burchard, J, Mao, M *et al.* (2003). Expression profiling reveals off-target gene regulation by RNAi. *Nat Biotechnol* **21**: 635–637.
36. Grimm, D, Streetz, KL, Jopling, CL, Storm, TA, Pandey, K, Davis, CR *et al.* (2006). Fatality in mice due to oversaturation of cellular microRNA/short hairpin RNA pathways. *Nature* **441**: 537–541.
37. Stärck, L, Popp, K, Pircher, H and Uckert, W (2014). Immunotherapy with TCR-redirected T cells: comparison of TCR-transduced and TCR-engineered hematopoietic stem cell-derived T cells. *J Immunol* **192**: 206–213.
38. Lassus, P, Rodriguez, J and Lazebnik, Y (2002). Confirming specificity of RNAi in mammalian cells. *Sci STKE* **2002**: pl13.
39. Pomerantz, JL, Denny, EM and Baltimore, D (2002). CARD11 mediates factor-specific activation of NF-kappaB by the T cell receptor complex. *EMBO J* **21**: 5184–5194.
40. Kim, DH and Rossi, JJ (2003). Coupling of RNAi-mediated target downregulation with gene replacement. *Antisense Nucleic Acid Drug Dev* **13**: 151–155.
41. Du, G, Yonekubo, J, Zeng, Y, Osisami, M and Frohman, MA (2006). Design of expression vectors for RNA interference based on miRNAs and RNA splicing. *FEBS J* **273**: 5421–5427.
42. Rosenberg, SA (2010). Of mice, not men: no evidence for graft-versus-host disease in humans receiving T-cell receptor-transduced autologous T cells. *Mol Ther* **18**: 1744–1745.
43. Yuan, B, Latek, R, Hossbach, M, Tuschl, T and Lewitter, F (2004). siRNA Selection Server: an automated siRNA oligonucleotide prediction server. *Nucleic Acids Res* **32**(Web Server issue): W130–W134.
44. Lu, ZJ and Mathews, DH (2008). Efficient siRNA selection using hybridization thermodynamics. *Nucleic Acids Res* **36**: 640–647.
45. Leisegang, M, Engels, B, Meyerhuber, P, Kieback, E, Sommermeyer, D, Xue, SA *et al.* (2008). Enhanced functionality of T cell receptor-redirected T cells is defined by the transgene cassette. *J Mol Med (Berl)* **86**: 573–583.
46. Morita, S, Kojima, T and Kitamura, T (2000). Plat-E: an efficient and stable system for transient packaging of retroviruses. *Gene Ther* **7**: 1063–1066.
47. Prévost-Blondel, A, Zimmermann, C, Stemmer, C, Kulmburg, P, Rosenthal, FM and Pircher, H (1998). Tumor-infiltrating lymphocytes exhibiting high ex vivo cytolytic activity fail to prevent murine melanoma tumor growth in vivo. *J Immunol* **161**: 2187–2194.